Modeling random telegraph signal noise in CMOS image sensor under low light based on binomial distribution*

Yu Zhang(张钰)[1,2,†], Xinmiao Lu(逯鑫淼)[2], Guangyi Wang(王光义)[1,2], Yongcai Hu(胡永才)[2], and Jiangtao Xu(徐江涛)[3]

[1] *Key Laboratory for RF Circuits and Systems (Hangzhou Dianzi University), Ministry of Education, Hangzhou* 310018, *China*
[2] *Institute of Electronics and Information, Hangzhou Dianzi University, Hangzhou* 310018, *China*
[3] *School of Electronics and Information Engineering, Tianjin University, Tianjin* 300072, *China*

(Received 6 February 2016; revised manuscript received 11 March 2016; published online 27 May 2016)

The random telegraph signal noise in the pixel source follower MOSFET is the principle component of the noise in the CMOS image sensor under low light. In this paper, the physical and statistical model of the random telegraph signal noise in the pixel source follower based on the binomial distribution is set up. The number of electrons captured or released by the oxide traps in the unit time is described as the random variables which obey the binomial distribution. As a result, the output states and the corresponding probabilities of the first and the second samples of the correlated double sampling circuit are acquired. The standard deviation of the output states after the correlated double sampling circuit can be obtained accordingly. In the simulation section, one hundred thousand samples of the source follower MOSFET have been simulated, and the simulation results show that the proposed model has the similar statistical characteristics with the existing models under the effect of the channel length and the density of the oxide trap. Moreover, the noise histogram of the proposed model has been evaluated at different environmental temperatures.

Keywords: random telegraph signal noise, physical and statistical model, binomial distribution, CMOS image sensor

PACS: 05.40.Ca, 85.40.Qx **DOI:** 10.1088/1674-1056/25/7/070503

1. Introduction

As the channel length of the metal–oxide–semiconductor field-effect transistor (MOSFET) continues to scale down to the nanoscale, the random telegraph signal (RTS) noise in the pixel source follower (SF) MOSFET has become an important issue to limit the sensitivity of the CMOS image sensor in the low light applications.[1–8] The physical origin of the RTS noise in SF is that the carriers are captured and released randomly by the traps located in the gate oxide or at the Si/SiO_2 interfaces. Since the RTS noise is not fully correlated in the time domain, it cannot be completely eliminated by the correlated double sampling (CDS) circuit of the CMOS image sensor (CIS).[2]

An accurate RTS noise model is conducive to eliminating the corresponding noise. Statistics is one of the most efficient ways to set up a noise model, and a great deal of effort has been made to model the RTS noise in the CMOS image sensor with the statistical analysis.[1,2,6–8] However, the proposed statistical models in the literature[1,6,8] are not connected with the physical mechanism of the RTS noise. References [2] and [7] used the statistical methods to describe the physical mechanism of the RTS noise. In Ref. [2], only the RTS noise caused by the single trap rather than by multiple traps was described by the statistical model, the CDS subtraction was utilized to calculate indirectly the standard deviation of the RTS noise caused by multiple traps. Reference [7] introduced the concept of the probability of trap occupancy (PTO) to represent the pixel output after CDS.

The above two statistical and physical models can depict the characteristics of the RTS noise caused by multiple traps efficiently. However, these models depend on the CDS circuit heavily, and cannot directly reflect the physical mechanism of the RTS noise caused by multiple traps. Therefore, a novel statistical model based on the binomial distribution is set up in this paper to depict directly the physical origin of the RTS noise caused by multiple traps in the pixel SF. The advantage of the proposed model is that it can directly and really describe the physical mechanism of the RTS noise caused by multiple traps, no matter weather the CDS circuit is considered or not. First of all, the number of the carriers captured or released by the multiple oxide traps in the unit time and the corresponding probability are derived from the binomial distribution. Then the output state and the corresponding probability of the first sample in CDS are obtained. Secondly, after the state transition probability between the two samples of CDS is obtained, the output state and the corresponding probability of the second sample in CDS can be inferred from the state transition probability in the unit time. Finally, the output state and the corresponding probability of the CDS output can be calculated from those of the two samples of CDS, and the standard devi-

*Project supported by the National Natural Science Foundation of China (Grant Nos. 61372156 and 61405053) and the Natural Science Foundation of Zhejiang Province of China (Grant No. LZ13F04001).

†Corresponding author. E-mail: yuzhang1978@163.com

© 2016 Chinese Physical Society and IOP Publishing Ltd

ation of the CDS output can be gained consequently.

The rest of the paper is organized as follows. Section 2 presents the proposed model of the RTS noise caused by multiple traps in the pixel SF. The simulation results and comparison with the existing statistical models are reported in Section 3. The conclusion is given in Section 4.

2. The proposed model of RTS noise in CIS

2.1. The structure of pixel and the CDS circuit in CIS

The structure and the time sequence of the four transistors (4T) pixel and the CDS circuit in CIS are shown in Fig. 1.[1,9–11] The CIS pixel comprises a transfer gate, a reset transistor, a row selector, a source follower, and a floating diffusion structure, named as TG, RS, SEL, SF, and FD, respectively, as shown in Fig. 1(a). S/H1 and S/H2 are two hold/samples of the CDS circuit. As shown in Fig. 1(b), during the pixel readout period, the row selector (SEL) is on. The RS and the S/H1 are enabled firstly to sample the reset voltage of the FD. After the charge transfer, the TG and the S/H2 are enabled to sample the image signal. The final CDS output of CIS is obtained by subtracting the reset sampled voltage from the signal sampled voltage.

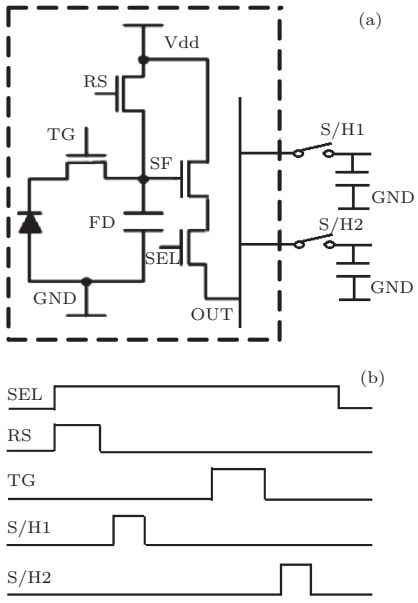


Fig. 1. (a) The structure of 4T pixel and (b) the time sequence of CDS circuit.

The process of random trapping and detrapping the carriers by the oxide trap in SF causes the RTS noise in the drain current, which is the main noise source of the CIS pixel in dark light applications. The CDS circuit can remove the correlated noise, such as the photodiode reset noise, but it fails to eliminate the RTS noise completely.[2] We make the same assumption like that in Refs. [1] and [2], i.e., the RTS noise in the pixel SF is the main source of the CIS noise under low light, and other noise can be ignored.

2.2. Modeling the RTS noise in pixel SF

The RTS noise caused by the single trap can be characterized by Fig. 2. The time of trapping the minority carriers is denoted as capture time τ_c, and that of releasing the minority carriers is denoted as emission time τ_e. The current levels in the capture time and the emission time are high and low, respectively, and the RTS states of the high and low current levels are denoted as states 1 and 0, respectively. The amplitude of the current level difference is denoted by ΔI_D. Let us take the electron as the minority carrier.

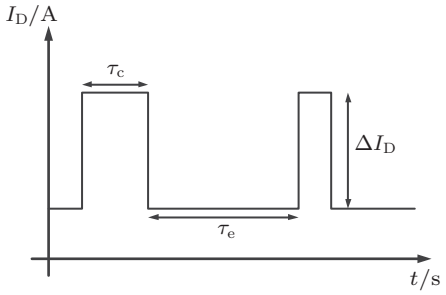


Fig. 2. The electrical characteristics caused by the single trap.

Since the current amplitude caused by the single trap is ΔI_D, the current amplitude caused by multiple traps can be represented by

$$I_{\Delta n} = \sum_{i=1}^{\Delta n} \Delta I_{Di}, \tag{1}$$

where $I_{\Delta n}$ is the current amplitude caused by multiple traps, Δn is the variable number of the electrons on the traps in unit time Δt and ΔI_{Di} is the current amplitude caused by one single electron of Δn electrons.

Equation (1) illustrates that the question of obtaining the RTS of the multiple traps can be transformed into the question of calculating the variable number of the electrons on the traps in the unit time and the current amplitude ΔI_{Di}. In order to set up the statistical model of the RTS current outputted by the CDS circuit, the following five steps in Fig. 3 are adopted. The details of the five steps are as follows.

Step 1 Getting the state transition probability and estimating the variable number of the electrons captured/released by the oxide traps in the unit time.

For the single trap, there are only two possible states, which are trapping or detrapping the electron. As shown in Table 1, state 1 indicates capturing the electron, and state 0 means releasing the electron. These two states do not occur at the same time, and they are independent of each other. Let P_1 be the probability that the trap energy level is occupied by the electron,

$$P_1 = f(E_T), \tag{2}$$

where $f(E_T)$ represents the Fermi–Dirac distribution function on the energy level E_T.

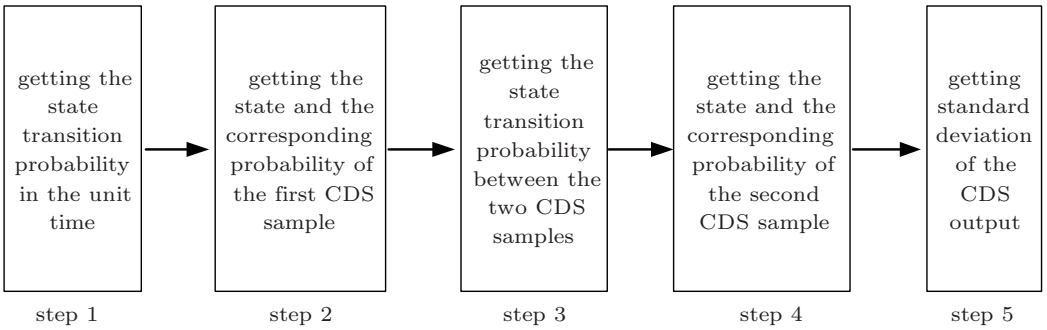


Fig. 3. The flowchart of the proposed RTS noise model.

Table 1. State and probability of trapping/detrapping the electron by the signal trap.

State	Probability
1	P_1
0	$1-P_1$

In this paper, we assume that one kind of trap contributes mostly to the RTS noise. Because the trap energy levels are the same, the probabilities of trapping/detrapping the electron/hole on the different trap energy levels are the same. According to the definition of the binomial distribution, the number of multiple traps occupied by the electrons can be represented by the binomial distribution, namely,

$$P_x(x=i) = C_N^i P_1^i (1-P_1)^{N-i}, \quad i = 0,1,2,\ldots,N, \tag{3}$$

where i is the number of traps occupied by the electrons, x is the state of i, P_x is the probability of x, and the total number of multiple traps is denoted by N.

Let the current time be t_n, the next time be t_{n+1}, and $\Delta t = t_{n+1} - t_n$, $n = 0,1,2,\ldots$. Figure 4 shows the state transition of the electron/hole captured by the trap energy level in the unit time Δt. If the electron/hole is captured by the trap energy level at the current time t_n, then the electron/hole is either released from the trap or is still captured by the trap at the next time t_{n+1}. Only the electrons/holes released by the trap energy level at time t_{n+1} make a contribution to the RTS current, while the electrons/holes still captured by the trap energy level at time t_{n+1} cannot cause the RTS current.

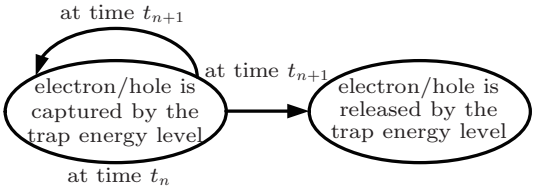


Fig. 4. The state transition of the electron/hole captured by the trap energy level in the unit time.

Let $x(l)$ be the RTS state at time l, the state transition probabilities from time t_n to time t_{n+1} are as follows:

$$P(x(t_{n+1}) = 1/x(t_n) = 0) = \frac{1}{[\tau_e/\Delta t]}, \tag{4}$$

$$P(x(t_{n+1}) = 0/x(t_n) = 1) = \frac{1}{[\tau_c/\Delta t]}, \tag{5}$$

where $[\cdot]$ means obtaining the integer part. The unit time Δt is the basic time unit of τ_e and τ_c. For example, if $\tau_e = 2.5\times10^{-3}$ s, then $\Delta t = 1\times10^{-3}$ s.

Let P_{10} and P_{11} be the probabilities of releasing the electron from the trap energy level originally occupied by the electron in the unit time Δt and keeping the electron on the trap energy level originally occupied by the electron in the unit time Δt, respectively. Let P_{01} and P_{00} be the probabilities of trapping the electron to the trap energy level originally occupied by the hole in the unit time Δt and keeping the hole on the trap energy level originally occupied by the hole in the unit time Δt, respectively. Then

$$P_{10} = P(x(t_{n+1}) = 0/x(t_n) = 1), \quad P_{11} = 1 - P_{10}, \tag{6}$$

$$P_{01} = P(x(t_{n+1}) = 1/x(t_n) = 0), \quad P_{00} = 1 - P_{01}. \tag{7}$$

Moreover, the events of trapping and detrapping the carriers by each trap energy level are independent. As a result, the variable number of the electrons/holes on the multiple traps can also be considered as following the binomial distribution. The state and probability of releasing the electrons from the trap energy level originally occupied by the electrons are as follows:

$$P_y(y=j) = C_i^j P_{10}^j P_{11}^{i-j}, \quad j = 0,1,2,\ldots,i, \tag{8}$$

where the number of electrons released from the trap energy level originally occupied by the electrons is denoted by j, y is the possible state of j, and P_y is the probability of state y.

Similarly, the state and probability of trapping the electrons to the trap energy level originally occupied by the holes are obtained as follows:

$$P_z(z=k) = C_{N-i}^k P_{01}^k P_{00}^{N-i-k}, \quad k = 0,1,2,\ldots,N-i, \tag{9}$$

where the number of electrons captured to the trap energy level originally occupied by the hole is indicated by k, the possible state of k is z, and P_z is the probability of state z.

Step 2 Getting the state and the corresponding probability of the first CDS sample.

Let $\Delta n = u = k - j$, then the state and probability of u can be written as

$$P_u(u = k-j) = P_x(x = i) \times P_y(y = j) \times P_z(z = k),$$
$$k - j = -N, -(N-1), -(N-2), \ldots, N, \quad (10)$$

where the variable number of the electrons on the multiple traps in the unit time is denoted by u, namely, the first CDS sample state, and P_u is the probability of state u.

In order to connect the above mathematical description with the physical mechanism of the RTS noise, the current amplitude caused by the single trap is calculated by[1]

$$\Delta I_{\mathrm{D}} = \frac{\eta g_{\mathrm{m}}}{C_{\mathrm{OX}}} \times \frac{q}{WL} \times \left(1 - \frac{x_{\mathrm{t}}}{t_{\mathrm{OX}}}\right), \quad (11)$$

where g_{m} is the MOSFET transconductance, W and L are the width and length of the MOSFET, C_{OX} is the MOSFET gate oxide capacitance, x_{t} is the distance between the trap and the Si/SiO_2 interface, t_{OX} is the gate oxide thickness, q is the elementary charge, and η is the fabrication process constant.

The trap number and the trap spatial location follow the Poisson distribution[2]

$$f(N) = \frac{N_{\mathrm{t}}^N}{N!} \mathrm{e}^{-N_{\mathrm{t}}}, \quad (12)$$

where $f(N)$ is the distribution function of the trap number or the trap spatial location, and N_{t} denotes the average trap number in the oxide volume or the average distance between the trap and the SiO_2 surface.

According to Eq. (12), the distance between the trap and the SiO_2 surface of every electron in Δn is different, so the current amplitude caused by every electron is different. The current amplitude caused by state u in Eq. (10) can be acquired by Eq. (1).

Step 3 Getting the state transition probability between the two CDS samples.

According to Refs. [2] and [10], the state transition probability in time t can be obtained by

$$P_{\mathrm{tr_00(t)}} = \frac{\tau_{\mathrm{e}}}{\tau_{\mathrm{e}} + \tau_{\mathrm{c}}} + \frac{\tau_{\mathrm{c}}}{\tau_{\mathrm{e}} + \tau_{\mathrm{c}}} \exp\left[-\left(\frac{1}{\tau_{\mathrm{e}}} + \frac{1}{\tau_{\mathrm{c}}}\right) t\right], \quad (13)$$
$$P_{\mathrm{tr_11(t)}} = \frac{\tau_{\mathrm{c}}}{\tau_{\mathrm{e}} + \tau_{\mathrm{c}}} + \frac{\tau_{\mathrm{e}}}{\tau_{\mathrm{e}} + \tau_{\mathrm{c}}} \exp\left[-\left(\frac{1}{\tau_{\mathrm{e}}} + \frac{1}{\tau_{\mathrm{c}}}\right) t\right], \quad (14)$$

where $P_{\mathrm{tr_00}}$ is the transition probability from state 0 to state 0 in time t, $P_{\mathrm{tr_11}}$ is the transition probability from state 1 to state 1 in time t, and t is the time interval of the two CDS samples.

Similar to Eqs. (8) and (9), the number of the electrons that change the state in time t and the corresponding probability can be obtained as

$$P_v(v = m) = C_i^m \left(1 - P_{\mathrm{tr_00}}(t)\right)^m P_{\mathrm{tr_00}}(t)^{i-m},$$
$$m = 0, 1, \ldots, i, \quad (15)$$
$$P_w(w = n) = C_{N-i}^n \left(1 - P_{\mathrm{tr_11}}(t)\right)^n P_{\mathrm{tr_11}}(t)^{N-i-n},$$
$$n = 0, 1, \ldots, N-i, \quad (16)$$

where m is the number of the electrons that have changed from state 0 to state 1 in time t, and n is the number of the electrons that have changed from state 1 to state 0 in time t.

Step 4 Getting the state and the corresponding probability of the second CDS sample.

At time t, there are totally $N - i - n + m$ oxide traps occupied by the electrons, while $i - m + n$ oxide traps are not occupied by the electrons. Let $e = N - i - n + m$ and $f = i - m + n$. According to Eqs. (4)–(9), the variable numbers of the electrons on the oxide traps and the corresponding probabilities in the unit time Δt can be obtained as follows:

$$P_{yy}(yy = jj) = C_{\mathrm{e}}^{jj} P_{10}^{jj} (1 - P_{10})^{e-jj}, \quad jj = 0, 1, \ldots, e, \quad (17)$$
$$P_{zz}(zz = kk) = C_f^{kk} P_{01}^{kk} (1 - P_{01})^{f-kk}, \quad kk = 0, 1, \ldots, f, \quad (18)$$

where jj and kk are the variable numbers of the electrons on the oxide traps in the unit time Δt, yy and zz are the states of jj and kk, and P_{yy} and P_{zz} are the probabilities of jj and kk, respectively.

Thus, the second sample output and the corresponding probability can be obained as

$$P_q(q = kk - jj) = P_x(x = i) \times P_v(v = m)$$
$$\times P_w(w = n) \times P_{yy}(yy = jj) \times P_{zz}(zz = kk),$$
$$kk - jj = -2N, -(2N-1), -(2N-2), \ldots, 2N. \quad (19)$$

Step 5 Getting the standard deviation of the CDS output.

Processed by the CDS circuit in Fig. 1, the state and the corresponding probability of the CDS output can be written as

$$P_o(o = q - u) = P_u(u) \times P_q(q),$$
$$q - u = -3N, -(3N-1), \ldots, 3N, \quad (20)$$

where o is the output state of the CDS circuit, and P_o is the probability of state o. The corresponding current amplitude I_o can be obtained by the similar method in step 2.

For the RTS noise analysis, we calculate the standard deviation of the CDS output

$$\sigma_o = \sqrt{\sum_o (I_o)^2 \times P_o(o) - \left(\sum_o (I_o) \times P_o(o)\right)^2}. \quad (21)$$

3. Simulation results and comparison

3.1. Simulation setting

We use simulation tool Matlab 2013. Both the trap number and the trap spatial location follow the Poisson distribution. The average distance between the trap and the surface of SiO_2 is set to 20 nm. The N_{t} in Eq. (12) is written as

$$N_{\mathrm{t}} = \int_{\Omega} n_{\mathrm{t}}(r)\, \mathrm{d}r, \quad (22)$$

where $n_{\mathrm{t}}(r)$ is the oxide trap density in the MOSFET, and Ω is the oxide volume in the source follower MOSFET.

Inspired by the assumption in Ref. [2] that the random traps follow a uniform distribution in energy, we set the density of the oxide trap in this paper to be 4×10^{16} cm$^{-3}\cdot$ eV^{-1} and 4×10^{17} cm$^{-3}\cdot$eV^{-1}. The distribution energy range of 0.1 μm channel width is set to be 2 eV.

On the other hand, the time interval of the two CDS samples in Eqs. (13) and (14) is set as 4 μs. According to Refs. [1], [2], and [11], τ_e and τ_c can be obtained by

$$\frac{\tau_e}{\tau_c} = \frac{1}{g}\exp\left[\frac{-(E_T - E_F)}{k_B T}\right], \tag{23}$$

$$\tau_e = \frac{\exp\left(\dfrac{\Delta E_B + \Delta E_{CT}}{k_B T}\right)}{T^2 \sigma \eta}, \tag{24}$$

where E_F is the Fermi energy level, E_T is the trap energy level, T is the temperature, k_B is the Boltzman constant, g is the trap degeneracy factor, g is assumed as 1,[2] Δ is the activation energy, Δ_T is the difference between the conduction band energy level and the trap energy level, and σ is the trap capture cross section.

Consulting the parameters in Refs. [2], and [10]–[13], in this paper, we set part parameters as follows. The 180-nm, 90-nm, and 50-nm devices have oxide thicknesses of 5 nm, 4.5 nm, and 2 nm, respectively. The channel width is set to 0.1 μm, ΔE_B is set as 0.186 eV, and σ equals to 9.9×10^{-23} m^2. The parameters η, g_m, and C_{OX} are set as constants.

After all the parameters are set, three cases are simulated: 1) with a high density of the oxide trap, the CDS output standard deviation with different channel lengths, 2) with a low density of the oxide trap, the CDS output standard deviation with different channel lengths, 3) the CDS output standard deviation at different temperatures.

3.2. Simulation results

Two state-of-the-art physical and statistical modeling methods in Refs. [2] and [7] are compared with the proposed modeling method. However, protocols to set up the RTS noise model and the corresponding parameters in these three methods are different, so it is difficult to compare the accurate data of the three methods, thus we compare the distribution rules of the RTS noise histograms of the three methods like Woo did in Ref. [2].

Figure 5 illustrates the RTS noise effect as the MOS devices scale down, namely, the histograms of the CDS output standard deviation simulated with the 180-nm, 90-nm, and 50-nm devices. The channel widths of these devices are 0.1 μm, and the density of the oxide trap is set to 4×10^{17} cm$^{-3}\cdot$eV^{-1}. Thus, the average trap numbers are 72, 32.4, and 8 in the oxides of the 180-nm, 90-nm, and 50-nm devices, respectively. The temperature is set to 300 K, ΔE_{CT} is set to 0.882 eV, and the difference between the conduction band energy level and the Femi energy level is set to 0.867 eV. One hundred thousand pixels in every device dimension are sampled to generate the RTS noise histogram in Matlab 400 bins.

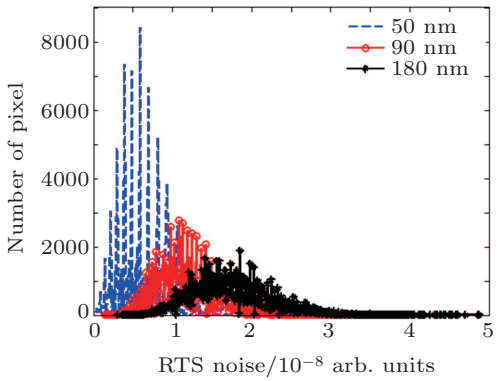


Fig. 5. (color online) RTS noise histograms of the devices with different channel lengths when the density of the oxide trap is set to 4×10^{17} cm$^{-3}\cdot$eV^{-1}.

Figure 6 shows the RTS histograms of the CDS output standard deviation simulated with the same device dimensions as those in Fig. 5. The density of the oxide trap is reduced to 4×10^{16} cm$^{-3}\cdot$eV^{-1}, and the average trap numbers are 7.2, 3.24, and 0.8 in the 180-nm, 90-nm, and 50-nm devices, respectively. The temperature is set to 300 K, ΔE_{CT} is set to 0.882 eV, and the difference between the conduction band energy level and the Femi energy level is set to 0.867 eV.

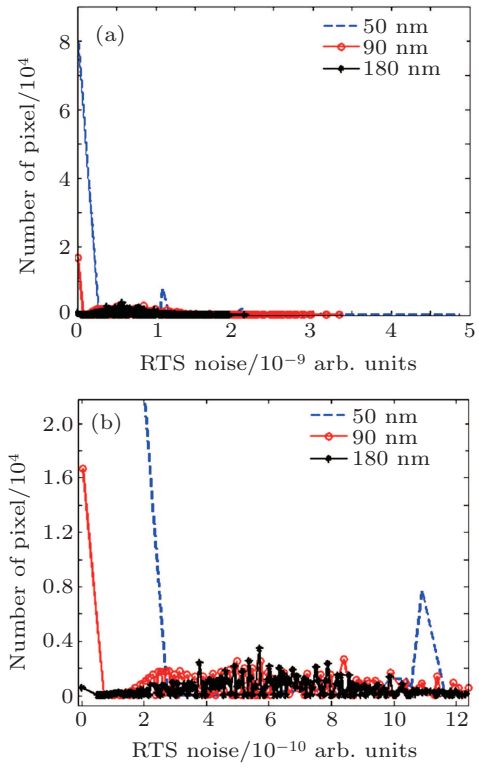


Fig. 6. (color online) RTS noise histograms of the devices with different channel lengths when the density of the oxide trap is set to 4×10^{16} cm$^{-3}\cdot$eV^{-1}: (a) the whole graph; (b) the partial enlarged detail.

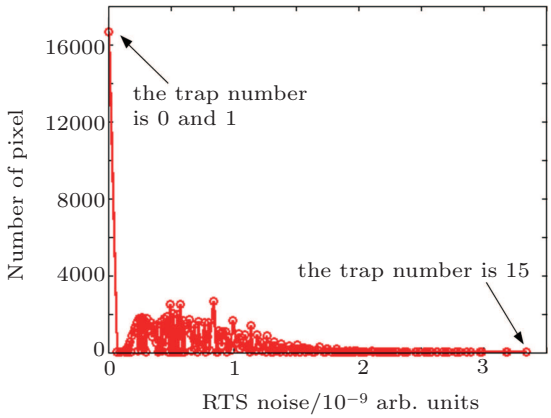


Fig. 7. (color online) RTS histograms of the quite sample and the noisy sample of the 90-nm device when the oxide trap density is set to 4×10^{16} cm^{-3}·eV^{-1}.

Figure 7 shows the quiet sample and the noisy sample in the RTS histogram of the 90-nm device, the trap density is set to 4×10^{16} cm^{-3}·eV^{-1}, and the average trap number is 3.24. The temperature is set to 300 K, and ΔE_{CT} is set to 0.882 eV, the difference between the conduction band energy level and the Femi energy level is set to 0.867 eV. It is shown in Fig. 7 that there are 15 traps in the oxide at the noisy sample, which are located in the tail part of the RTS histogram, and there is less than one trap in the oxide of the quiet sample.

Figure 8 is the simulation results of the standard deviation of the CDS output at different temperatures. The length of the device is set to 90 nm, the width of the device is 0.1 μm, the trap density is set to 4×10^{16} cm^{-3}·eV^{-1}, and the distribution energy range of 0.1 μm channel width is set to be 2 eV. So the average trap number is 3.24. The temperature is set to 300 K, 800 K and 1300 K respectively. The difference between the conduction band energy level and the Femi energy level is set to 0.867 eV. The E_T–E_F is set to 0.035 eV in Figs. 8(a) and 8(b), and −0.035 eV in Figs. 8(c) and 8(d).

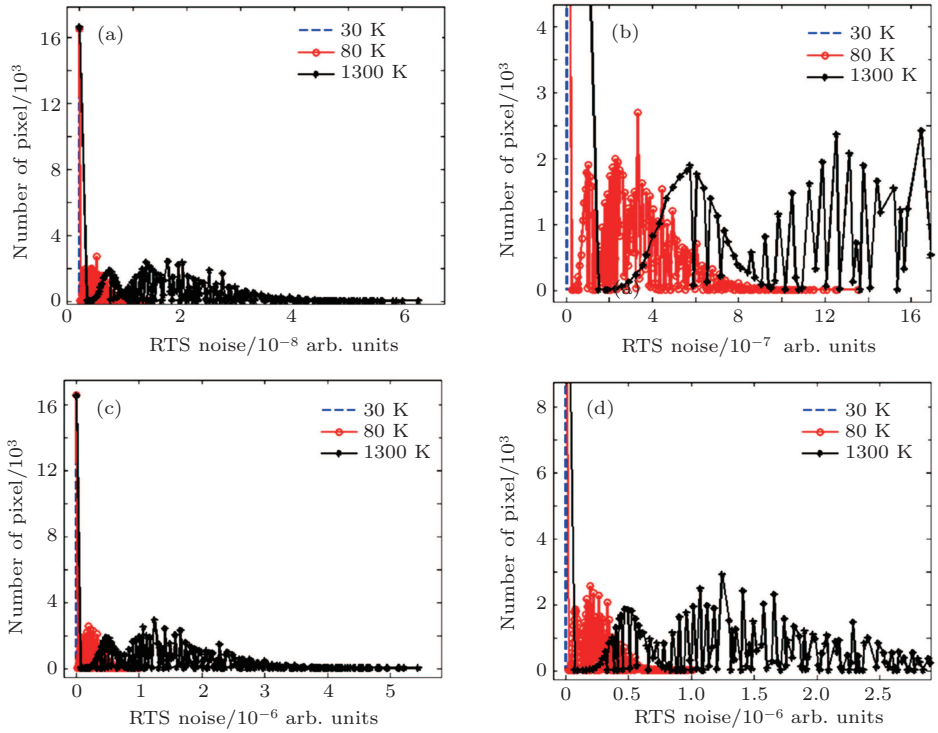


Fig. 8. (color online) RTS noise histograms at different temperatures when the density of the oxide trap is set to 4×10^{16} cm^{-3}·eV^{-1}. (a) RTS noise histograms at different temperature when $E_T - E_F > 0$; panel (b) shows a partial enlarged detail of panel (a). (c) RTS noise histograms at different temperature when $E_T - E_F < 0$; panel (d) shows a partial enlarged detail of panel (c).

3.3. Comparison

Table 2 shows a comparison of different modeling methods. It is indicated in Table 2 and Fig. 5 that the asymmetric distributions of the RTS noise in the three methods are similar to the $1/f$ noise, and the RTS noise tail distributions of the 180-nm device in Ref. [2] and the proposed method are longer than that of the short-channel device, because the trap number in the 180-nm device is larger than that of the short-channel device.

It can be seen from Table 2 and Fig. 6 that in Ref. [2] and the proposed method, the short-channel devices have a longer RTS noise tail distribution than the long-channel device. The simulation result in Fig. 6 is contrary to that in Fig. 5. With the decrease of the device size, the low density of the oxide trap makes the trap number in the oxide volume become smaller, or even close to 1, which enlarges the effect of the single RTS amplitude. It can also be interpreted as that the distance between the trap and the Si/SiO$_2$ interface becomes small as the device dimension is diminished.

Table 2. Comparison of the RTS noise histograms of different modeling methods.

	Ref. [2]	Ref. [7]	Proposed method
Asymmetric distributions	$1/f$ noise	$1/f$ noise	$1/f$ noise
Density of the oxide trap 4×10^{17} cm$^{-3}\cdot$eV^{-1}, channel length ↑	RTS noise tail distribution ↑	–	RTS noise tail distribution ↑
Density of the oxide trap 4×10^{16} cm$^{-3}\cdot$eV^{-1}, channel length ↑	RTS noise tail distribution ↓	–	RTS noise tail distribution ↓
$E_{\rm T}-E_{\rm F}>0$, temperature ↑	–	–	RTS noise tail distribution ↑
$E_{\rm T}-E_{\rm F}<0$, temperature ↑	–	–	RTS noise tail distribution ↑

It can be inferred from Table 2, Figs. 8(a) and 8(c) that the RTS noise will become stronger with the increase of the temperature when the device dimension and the density of the oxide trap are fixed. This simulation result can be explained as follows. With the increase of the temperature, the capture time and the release time of the oxide traps become shorter. In other words, the frequency of carriers trapping and detrapping becomes high, and the number of the electrons which change state in the same time increases.

4. Conclusion

A novel physical and statistical model of the RTS noise in the pixel source follower of CIS based on the binomial distribution is proposed in this paper. One hundred thousand samples are simulated to verify this model, and the similar conclusion with the state-of-the-art statistical models can be acquired from the simulation results, i.e., the long channel device has the longer tail in the RTS noise histogram when the density of the oxide trap is high, while the short channel device has the longer tail in the RTS noise histogram in the case of low oxide trap density. The simulation results also illustrate that the longer tail in the RTS noise histogram will appear at the high environmental temperature if the device dimension and the density of the oxide trap are fixed. The proposed noise model supplies a possible approach to find the relationship among the RTS noise, the temperature, and the device dimension, which is of benefit to eliminate the RTS noise and improve the sensitivity of the CMOS image sensor.

In the future, we will design a detecting circuit for the RTS noise of CIS, and analyze the statistical characteristics of the RTS noise. The experimental data will be used to compare with the simulation results in this paper. These works will generate new theoretical innovation and enhance the noise performance of CIS.

References

[1] Martin-Gonthier P, Goiffon V and Magnan P 2012 *IEEE Trans. Electron. Dev.* **6** 1686

[2] Woo J M, Park H H, Hong S M, Chung I Y, Min H S and Park Y J 2009 *IEEE Trans. Electron. Dev.* **11** 2481

[3] Kim B C, Jeon J and Shin H 2009 *IEEE Trans. Electron. Dev.* **11** 2489

[4] Virmontois C, Goiffon V, Corbiere F, Magnan P, Girard S and Bardoux A 2012 *IEEE Trans. Nucl. Sci.* **6** 2872

[5] Goiffon V, Estribeau M, Marcelot O, Cervantes P, Magnan P, Gaillardin M, Virmontois C, Gonthier P M, Molina R, Corbiere F, Girard S, Paillet P and Marcandella C 2012 *IEEE Trans. Nucl Sci.* **6** 2878

[6] Zhang D, Ryu J and Nishimura T 2012 *IEICE Trans. Inf. Syst.* **2** 350

[7] Wang X Y, Rao P R, Mierop A and Theuwissen A J P 2006 *Proceedings of IEEE International Electron Devices Meeting* 1

[8] Leyris C, Martinez F, Valenza M, Hoffmann A, Vildeuil J C and Roy F 2006 *Proceedings of the 32nd European Solid-State Circuits Conference* 376

[9] Tan J, Buttgen B and Theuwissen A J P 2012 *IEEE Sens. J* **6** 2278

[10] Kirton M J and Uren M J 1989 *Adv. Phys.* **4** 367

[11] Feng W, Dou C M, Niwa M, Yamada K and Ohmori K 2014 *IEEE Electron. Dev. Lett.* **1** 3

[12] Qiu C, Sheng Z, Li L, Pang A, Wu A M, Wang X, Zou S C and Gan F W 2013 *Chin. Phys. B* **22** 024212

[13] Zhang L N, He J, Zhou W, Chen L and Xu Y W 2010 *Chin. Phys. B* **19** 047306